Metallophysics and Advanced Technologies
Металофіз. новітні технол.
Metallofiz. Noveishie Tekhnol.
2020, vol. 42, No. 10, pp. 1387–1400
https://doi.org/10.15407/mfint.42.10.1387
Reprints available directly from the publisher

PHASE TRANSFORMATIONS

PACS numbers: 05.10.Ln, 05.70.-a, 65.40.G-, 81.30.Bx, 81.30.Fb

Thermodynamic Prediction of Phase Composition of Transition Metals High-Entropy Alloys

A. B. Melnick, V. K. Soolshenko, and K. H. Levchuk

G. V. Kurdyumov Institute for Metal Physics, N.A.S. of Ukraine,
36 Academician Vernadsky Blvd.,
UA-03142 Kyiv, Ukraine

Compositions with minimal Gibbs free energy for single- and multi-phase high-entropy alloys (HEAs) containing Ni, Co, Fe, Cr, Cu, Al, Mn, Ti, Zr, V elements are developed using a developed thermodynamic approach. The phase compositions for some equiatomic HEAs are predicted and the influence of various factors on its formation are described. A correlation between theoretical and experimental data is obtained. Criteria for search of HEAs compositions favourable for formation of single-phase and multi-phase solid solutions are formulated.

Key words: thermodynamic prediction, high-entropy alloys, solid solution, intermetallic compounds.

Композиції з мінімальною вільною енергією Гіббса для однофазних і гетерофазних високоентропійних стопів (ВЕС), що містять Ni, Co, Fe, Cr, Cu, Al, Mn, Ti, Zr, V, одержані за допомогою розвинутого термодинамічного підходу. Спрогнозовано фазовий склад ряду еквіатомних ВЕС та описано вплив різних чинників на його формування. Одержано кореляцію розрахованих даних з експериментальними. Сформульовано критерії пошуку складів ВЕС, сприятливих для утворення як однофазних, так і багатофазних твердих розчинів.

Ключові слова: термодинамічне прогнозування, високоентропійні стопи, твердий розчин, інтерметалічні композити.

Corresponding author: Oleksiy Bronislavovych Melnick
E-mail: mel@imp.kiev.ua

Citation: A. B. Melnick, V. K. Soolshenko, and K. H. Levchuk, Thermodynamic Prediction of Phase Composition of Transition Metals High-Entropy Alloys, *Metallofiz. Noveishie Tekhnol.*, **42**, No. 10: 1387–1400 (2020), DOI: 10.15407/mfint.42.10.1387.

(Received August 20, 2020)

1. INTRODUCTION

The conception of high-entropy alloys (HEAs) is proposed by Yeh *et al.* in 2004 [1] and based on the idea that the high configurational entropy would stabilize the solid solution (*SS*) phase. HEAs are multicomponent (5 or more) bulk solid solutions, intermetallic or glasses with near equiatomic composition [1–5]. This can provide a large value of mixing entropy (ΔS_{mix}) for the formation homogeneous *SS* system. For regular solution:

$$\Delta S_{mix} = -k\sum_{i=1}^{n} c_i \ln(c_i), \qquad (1)$$

where c_i is the atomic fraction of i-th element, k is Boltzmann constant.

According to (1), the maximum effect of the entropy factor will be in the equiatomic case.

In recent years, high-entropy solid solutions (HESS) have attracted increasing attentions, because they exhibit special structure and unique properties. Many HEAs studies are devoted to the search for single-phase *SS* [6, 7].

The thermodynamic properties of alloy are very important for understanding of relative stability of single-phase *SS*. In concordance with thermodynamics, a system will be in a stable equilibrium state if it has the lowest Gibbs free energy. The difference between the Gibbs free energy of solid phase and liquid phase is

$$\Delta G = \Delta H - T\Delta S.$$

Here ΔH is the formation enthalpy, T—absolute temperature, ΔS—total entropy.

Many methods have been devised to estimate the formation enthalpies and other thermodynamic properties of alloys with a single solid solution phase:

1. First principles calculations, within the framework of density-functional theory combined with atomistic simulation techniques like ab-initio calculations, molecular dynamics simulations and Monte Carlo methods [8–13].
2. Solution thermodynamics is based on extrapolation of experimental data, as in the CALPHAD [14–16].
3. Semi-empirical Miedema's model, and empirical thermophysical parameters based on Hume–Rothery rules [17].

It should be noted that first principle calculations and atomistic simulation techniques have a high computational difficulties for multicomponent systems. The CALPHAD-method needs extensive database of experimental thermodynamic functions of multicomponent alloys. Various thermophysical parameters are proposed to predict formation of single phase solid solutions. Among them: mixing entropy ΔS_{mix} [18], mixing enthalpy ΔH_{mix} [18], differences of atomic sizes δr [18], $\Omega = T_m\Delta S_{mix}/|\Delta H_{mix}|$ [19], valence electron concentration [20], electronegativity difference $\delta\chi$ [21], the φ-parameter [22], elastic-strain energy [23] and other. An analysis of these parameters gives possibility to conclude whether the alloy will be in the state of solid solution. But such approach is semi-quantitative and does not allow optimizing the alloy composition. For more accurate estimations the Miedema-method has to be adapted. Takeuchi and Inoue [24] supposed that for multi-component glasses ΔG is proportional to free energy ΔG_{mix} of liquid phases mixing.

$$\Delta G_{mix} = \Delta H_{mix} - T\Delta S_{mix}.$$

Here ΔH_{mix} is an enthalpy of mixing.

In solid solutions, where atoms of different sizes occupy equivalent lattice positions, the additional energy of elastic interactions (ΔH_{el}) has to be taken into account. Since the crystal structure of 3*d* transition element depends on the number of valence electrons of the metal, the solution formation can leads to transformation one type lattice to other and the corresponding energy change—ΔH_{str} [25]:

$$\begin{aligned}\Delta H_{SS} &= \Delta H_{mix} + \Delta H_{el} + \Delta H_{str},\\ \Delta G_{SS} &= \Delta H_{mix} + \Delta H_{el} + \Delta H_{str} - T\Delta S_{mix}.\end{aligned} \tag{2}$$

Regular solution model has been adopted in order to simplify the calculation of (2) and minimization of ΔG on element concentrations [26]. Thus, it is possible to obtain the most stable multicomponent solutions.

In the case of formation of intermetallic compounds:

$$\Delta H_{inter} = \Delta H_{mix}, \quad \Delta G_{inter} = \Delta H_{mix}.$$

The ΔG_{ss} and ΔG_{inter} values have to be compared to determine what structural type is formed.

Since Cantor alloy [27], single-phase NiCoFeCr-based HEAs are the promising materials with high tensile ductility and fracture toughness [28]. Development of NiCoFeCr-based HEAs is continued by adding new elements into equiatomic NiCoFeCr basis for strengthening. The composition of the most stable HEA may be different from the equiatomic one because some additional contributions to entropy. To find the compositions of stable solid solutions including Ni, Co, Fe, Cr, Cu, Al, Mn, Ti, Zr, V elements, we minimize Gibbs free energies of investigated systems [29].

2. MODELING

Compositions for HEAs with minimal Gibbs free energy are obtained based on thermodynamic approach, developed in the article [26], where substitutional solid solutions are considered with the regular solution approximation. The parameters for expression 2 are determined as follows. The mixing enthalpy of multicomponent alloy consisting of n elements is [30]:

$$\Delta H_{mix} = \sum_{i,j=1 \quad i\neq j}^{n} c_i c_j \Omega_{ij}, \tag{3}$$

where Ω_{ij}-parameter characterises the interaction between i and j elements of the regular solution, $\Omega_{ij} = 4\Delta H_{mix}^{ij}$, c_i is atomic fraction of i component. ΔH_{mix}^{ij} is mixing enthalpy for binary liquid equiatomic alloy. The values ΔH_{mix}^{ij} are taken from [31].

The elastic distortion energy in the solid solution ΔH_{el} is:

$$\Delta H_{el} = \sum_{i=1}^{n} c_i B_i \frac{[V_i(T) - V(T)]^2}{2V_i(T)}. \tag{4}$$

Here $V(T)$ is the average volume of atom of the alloy, $V_i(T)$ is atomic volume and B_i is bulk modulus of i-th element:

$$V_i(T) = V_{0i}[1 + 3\alpha_i(T - T_0)],$$

α_i is linear expansion coefficient for the i component, $T_0 = 293$ K,

$$V(T) = \frac{\sum_{i=1}^{n} c_i B_i V_i(T)}{\sum_{i=1}^{n} c_i B_i}.$$

Using the rule of mixtures the effective melting temperature of n-elements solid solution T_m is approximately estimated as:

$$T_m \approx \sum_{i=1}^{n} c_i T_m^i,$$

where T_m^i is melting temperature of i element.

The ΔH_{str} is structural enthalpy of these solid solutions depends on average number of valence electrons Z. It is written as:

$$Z = \sum_{i=1}^{n} c_i z_i,$$

where z_i is number of valence electrons for i-th element.

Based on band-structure calculations and empirical curves of variation in the enthalpy of b.c.c., f.c.c., and h.c.p. crystal structures with respect to Z [32], we obtained $\Delta H_{str}(Z)$ for solid solution.

Then Gibbs free energy for SS can be written as:

$$\Delta G_{\substack{ss \\ i=1-n}}(c_i) = \sum_{i,j=1 \quad i \neq j}^{n} c_i c_j \Omega_{ij} + \sum_{i=1}^{n} c_i B_i \frac{[V_i(T_m) - V(T_m)]^2}{2V_i(T_m)} + \\ + \Delta H_{str}(Z) - kT_m \sum_{i=1}^{n} c_i \ln(c_i). \tag{5}$$

And for intermetallic compounds:

$$\Delta G_{\substack{\text{int} \\ i=1-n}}(c_i) = \sum_{i,j=1 \quad i \neq j}^{n} c_i c_j \Omega_{ij}. \tag{6}$$

A minimization of ΔG is carried out using the Monte Carlo method. The values of the constants α_i, V_{0i}, B_i, T_m^i, Z_i in expressions (5), (6) are taken from tables [33]. The minimums of ΔG correspond to the compositions of stable alloys. To analyse the state of alloys, a number parameters are used: ΔG, ΔH_{mix}, ΔH_{el}, ΔS_{mix}, T_m, $\Omega = T_m \Delta S_{mix}/|\Delta H_{mix}|$,

$$\delta = \sqrt{\sum_{i=1}^{n} c_i (1 - r_i/\bar{r})^2},$$

where $r_i = \sqrt[3]{V_{0i}}$, $\bar{r} = \sum_{i=1}^{n} c_i r_i$.

3. RESULTS AND DISCUSSION

The calculation results are summarized in tables for different element combinations (in Table 1 for equiatomic compositions and Table 2 for SS with minimal Gibbs free energy). Optimized SS compositions are significantly different from equiatomic ones. The differences of compositions are illustrated by Gibbs free energy-composition diagrams for ternary and quasi-ternary alloy systems (Fig. 1 and Fig. 2). It should be noted that in the case of solid solutions, taking into account ΔH_{str} significantly changes the Gibbs energy [36].

If we consider the system consisting of four basic elements (Ni, Co, Fe, Cr), we can observe the existence of a wide range of concentrations around the equiatomic point where a single solid solution will be formed (Fig. 1, Table 1 and Table 2). CALPHAD calculations with experimental verifications [28] indicate the same result. What elements can be added to the basic composition to reduce Gibbs energy and not destroy the solid solution?

Let's explore this question. If we examine equiatomic compositions (see Table 1), the additions of Al, Mn, Ti, Zr, V to the base elements decreases the Gibbs energy. While Cu increase it. ΔH_{mix}, δ, Ω parameters play a special role in formation of solid solutions. Solid solution is crystallized, when $\delta < 6\%$ and $\Delta H_{mix} > -10$ kJ/mol [34]. According to [35], $\Omega \geq 1.1$ and $\delta \leq 6.6\%$ should be considered as a criterion for forming solid-solution phase. Thus, it can be concluded that the (NiCoFeCr, NiCoFeCrCu, NiCoFeCrAl, NiCoFeCrMn, NiCoFeCrV, CoFeCrCuMn, NiFeCrMnTi, NiCoFeMnV, NiCoCrMnV, NiCoFeCrCuTi, NiFeCrCuAlMn, NiCoFeCrCuAl, NiCoFeCrCuMn, NiCoFeCrCuAlV, NiCoFeCrAlMnV) equiatomic compositions may form stable solid solutions. Addition of Zr, Ti to the base elements (NiCoFeCrZr, NiCoFeCrTi) leads to a significant decrease in Gibbs energy, but at the same time the energy of elastic deformation increases to a level incompatible with the existence of a solid solution.

TABLE 1. Calculated parameters ΔG_{ss}, ΔH_{mix}, ΔH_{el}, δ, Ω , ΔS_{mix}, T_m, ΔH_{str} for equiatomic solid solutions.

No.	Alloys	ΔG_{ss}	ΔH_{mix}	ΔH_{el}	ΔH_{str}	δ	Ω	ΔS_{mix}	T_m
		kJ/mol				%		J/(mol·K)	K
1	NiCoFe	–11.802	–1.333	0.5231	5.166	1.068	12.119	9.135	1769
2	NiCoCr	–17.200	–4.889	0.2988	4.666	1.373	3.535	9.135	1892
3	CoFeCr	–15.351	–2.667	0.3492	4.500	1.134	6.576	9.135	1920
4	NiFeCr	–15.180	–4.444	0.5111	6.167	1.322	3.918	9.135	1906
5	NiCoFeCr	–19.221	–3.750	0.4755	5.625	1.306	5.753	11.527	1872
6	NiCoFeCrCu	–13.884	3.200	0.6889	5.900	1.241	7.398	13.382	1769
7	NiCoFeCrAl	–20.952	–12.320	9.959	3.980	5.281	1.829	13.382	1684
8	NiCoFeCrMn	–21.172	–4.160	1.400	5.700	1.454	5.7941	13.382	1801
9	NiCoFeCrTi	–24.766	–16.320	13.984	2.800	6.153	1.5461	13.382	1886
10	NiCoFeCrZr	–20.252	–22.720	25.390	2.800	10.21	1.132	13.382	1923
11	NiCoFeCrV	–28.083	–8.960	3.752	3.000	2.896	2.888	13.382	1934
12	CoFeCrCuMn	–13.219	4.160	1.035	4.700	1.092	5.556	13.382	1727
13	NiFeCrMnTi	–20.167	–13.280	13.279	4.400	5.821	1.850	13.382	1836
14	NiCoFeMnV	–28.377	–8.960	4.293	0.400	2.912	2.691	13.382	1801
15	NiCoCrMnV	–26.770	–9.119	4.348	3.100	2.897	2.752	13.382	1875
16	NiCoFeCrCuTi	–19.588	–8.444	11.639	4.000	5.685	3.172	14.898	1798
17	NiFeCrCuAlMn	–20.625	–5.111	7.830	0.317	4.614	4.629	14.898	1588
18	NiCoFeCrCuAl	–21.870	–4.778	8.233	–1.017	4.867	5.081	14.898	1630
19	NiCoFeCrCuMn	–18.609	1.444	1.263	4.416	1.346	17.81	14.898	1727
20	NiCoFeCrCuAlV	–24.678	–7.755	8.808	1.914	4.716	3.564	16.179	1709
21	NiCoFeCrAlMnV	–41.711	–13.469	9.005	–9.228	4.661	2.080	16.179	1732

TABLE 2. Calculated parameters ΔG_{ss}, ΔH_{mix}, ΔH_{el}, δ, Ω , ΔS_{mix}, T_m, ΔH_{str} for solid solutions with minimal Gibbs formation energy.

No.	Alloys	ΔG_{ss}	ΔH_{mix}	ΔH_{el}	ΔH_{str}	δ	Ω	ΔS_{mix}	T_m
		kJ/mol				%		J/(mol·K)	K
1	$Ni_{36.3}Co_{27.4}Fe_{35.3}$	–11.930	–1.452	0.558	5.003	1.100	11.046	9.067	1769
2	$Ni_{15.4}Co_{12.8}Cr_{71.8}$	–26.742	–4.566	0.249	6.561	1.299	2.956	6.561	2057
3	$Co_{20}Fe_{20}Cr_{60}$	–26.235	–2.560	0.215	–7.900	1.027	6.246	7.901	2024
4	$Ni_{17.1}Fe_{15.8}Cr_{67.1}$	–27.171	–3.853	0.269	–8.947	1.127	3.800	7.161	2044
5	$Ni_{11}Co_{10.6}Fe_{12.1}Cr_{66.3}$	–29.117	–3.645	0.254	–8.599	1.157	4.698	8.387	2042
6	$Ni_{11}Co_{9.9}Fe_{12.9}Cr_{66.1}Cu_{0.1}$	–29.145	–3.5467	0.254	–8.602	1.145	4.865	8.452	2041
7	$Ni_{24.2}Co_{13.7}Fe_{10.9}Cr_{31.3}Al_{19.9}$	–37.049	–12.969	9.953	–11.904	5.238	1.706	12.8227	1726
8	$Ni_{9.5}Co_{8.2}Fe_{10.2}Cr_{55.1}Mn_{17}$	–32.078	–2.570	1.000	–9.538	1.155	8.157	10.7350	1953
9	$Ni_{25.5}Co_{13.4}Fe_{11}Cr_{18}Ti_{32.1}$	–38.487	–22.329	21.140	–13.166	7.105	1.0801	12.7543	1892
10	$Ni_{16.6}Co_{12.2}Fe_{13.1}Cr_{43.5}Zr_{14.6}$	–32.493	–15.969	18.416	–10.600	8.940	1.5232	12.1730	1999
11	$Ni_{21}Co_{12}Fe_{9.9}Cr_{17.3}V_{39.8}$	–41.404	–11.978	5.814	–10.603	3.424	2.0560	12.3163	2000
12	$Co_{14}Fe_{18.5}Cr_{46.9}Cu_{0.1}Mn_{20.5}$	–29.748	–1.267	0.983	–9.144	0.994	16.033	10.5955	1918
13	$Ni_{30.6}Fe_{11}Cr_{15.8}Mn_{13.6}Ti_{29}$	–38.396	–19.990	18.912	–13.931	6.752	1.1690	12.6963	1841
14	$Ni_{20.3}Co_{11.5}Fe_{9.5}Mn_{12}V_{46.7}$	–40.521	–12.553	6.095	–11.524	3.492	1.7950	11.6918	1928
15	$Ni_{22.6}Co_{12.3}Cr_{16}Mn_{10.9}V_{38.2}$	–41.551	–11.746	5.880	–11.346	3.393	2.0717	12.4415	1956
16	$Ni_{25.4}Co_{12.8}Fe_{11}Cr_{18}Cu_{0.5}Ti_{32.3}$	–38.545	–22.118	21.204	–13.199	7.105	1.1043	12.9221	1890
17	$Ni_{29.5}Fe_{9.5}Cr_{18}Cu_{0.7}Al_{20.7}Mn_{21.6}$	–39.039	–14.488	10.265	–13.675	5.170	1.4590	13.1720	1605
18	$Ni_{25}Co_{12}Fe_{11.3}Cr_{30.8}Cu_{0.5}Al_{20.4}$	–37.073	–12.909	10.154	–12.029	5.276	1.7260	12.9780	1717
19	$Ni_{6}Co_{5.9}Fe_{16.8}Cr_{47}Cu_{0.1}Mn_{24.2}$	–31.344	–1.472	1.106	–9.734	1.013	14.430	11.1460	1906
20	$Ni_{25.9}Co_{17}Fe_{7.3}Cr_{10.3}Cu_{0.3}Al_{15.8}V_{23.4}$	–44.125	–17.624	11.177	–12.329	5.141	1.4382	14.3440	1767
21	$Ni_{25.5}Co_{11}Fe_{6.9}Cr_{9.3}Al_{10.9}Mn_{10.1}V_{26.3}$	–46.270	–16.019	9.260	–12.376	4.601	1.6930	15.1410	1792

Using optimization procedure we obtain alloys that are superior in energy stability as compared with equiatomic ones (Table 2).

They differ in composition from equiatomic HEAs. Let us consider these differences. If we consider the relationship between the basic components (Ni, Co, Fe, Cr) in optimized alloys, the element predominance (Cr in system 2–8, 10, 12, 18, 19 (Table 2)); (Ni in system 9, 11, 13–15, 20, 21 (Table 2)) are observed. Optimization of compositions leads to a significant decrease in Gibbs energy mainly due to a change in the energy of elastic distortions, enthalpy of mixing or melting temperature.

The Gibbs free energy change for the formation of solid solution (5) has to be compared with the energy of formation of intermetallic compound (6) in order to determine what phases are preferable. To do this,

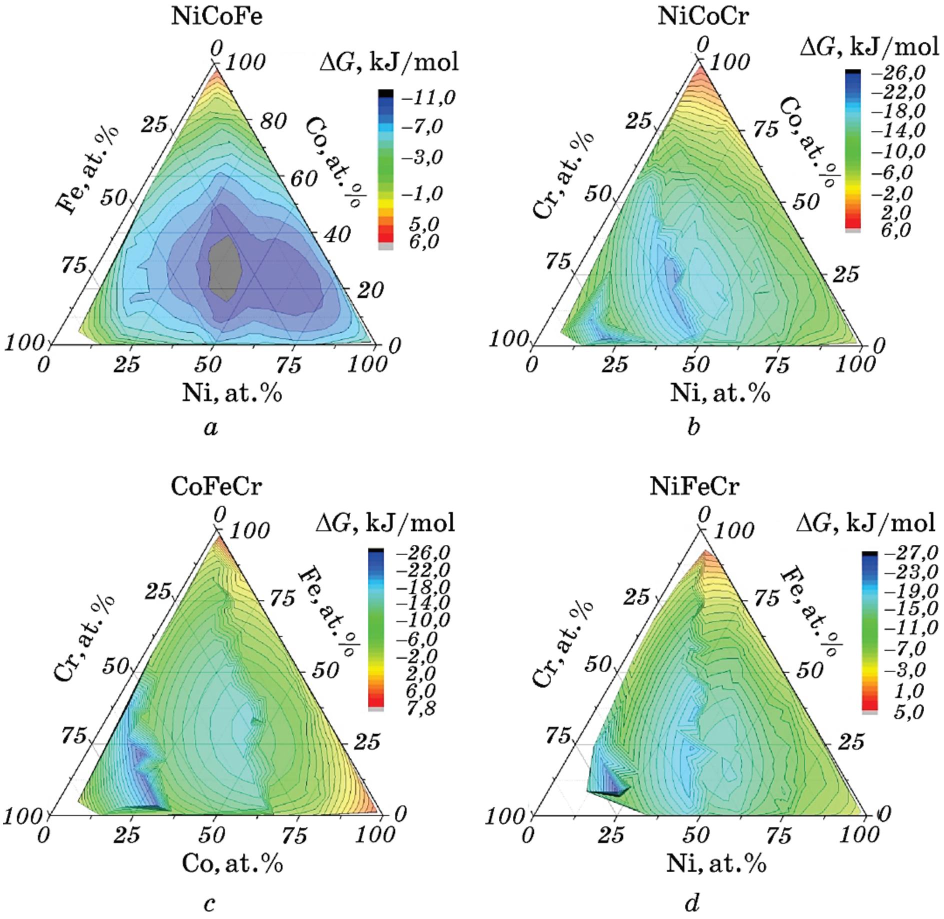

a *b* *c* *d*

Fig. 1. The calculated Gibbs formation energy of solid solutions (ΔG_{ss}) for ternary Ni–Co–Fe (*a*), Ni–Co–Cr (*b*), Co–Fe–Cr (*c*), Ni–Fe–Cr (*d*) alloy systems.

we calculated intermetallic compounds with minimal formation energies ΔG_{int} (6) for the systems under consideration. The calculation results are presented in the Table 3 together with experimental data. For each equiatomic alloy, the compositions of the solid solution (*ssm*) and the intermetallic compound (*intm*) with the minimum formation energy are determined.

The Gibbs formation energy is also obtained for the residual solid solutions that can be formed during crystallization of a solid solution (*ssm_ss*) or intermetallic (*intm_ss*—only for resistant compound). By analyzing the data, the following correlations can be seen: when ΔG_{ssm} and ΔG_{ssm_ss} is much less than ΔG_{intm}, a single solid solution or solutions

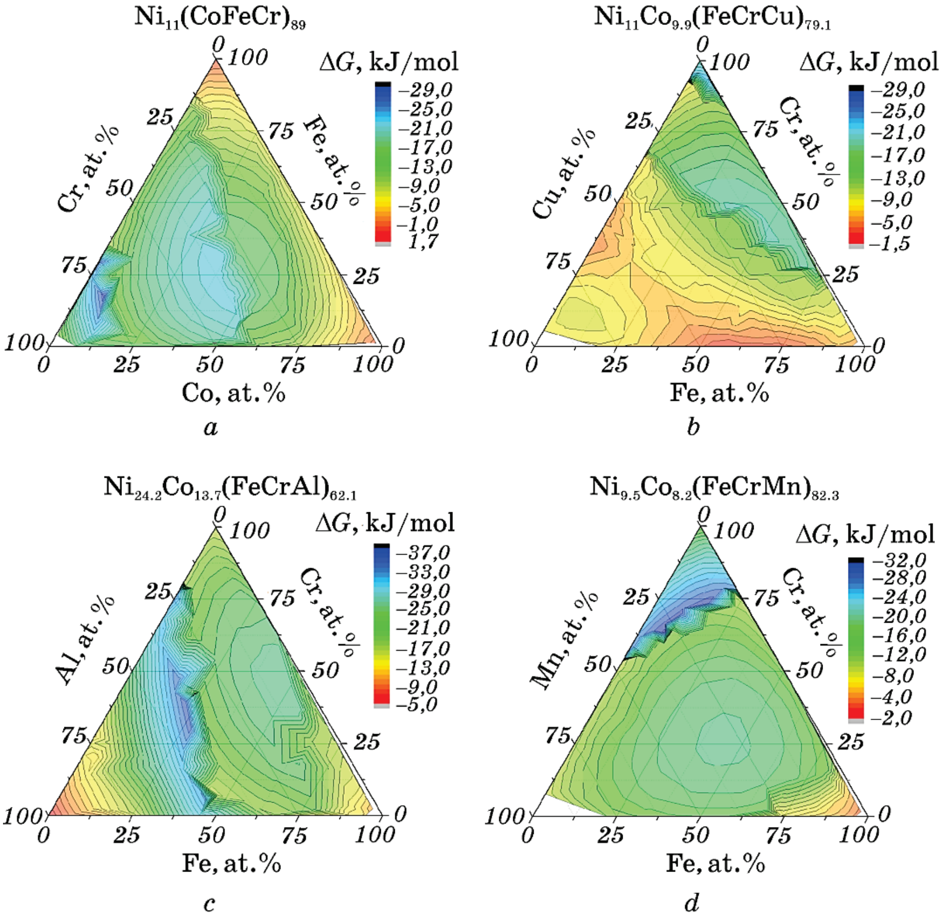

a *b* *c* *d*

Fig. 2. The calculated Gibbs formation energy of solid solutions (ΔG_{ss}) for quasi-ternary $Ni_{11}(CoFeCr)_{89}$ (*a*), $Ni_{11}Co_{9.9}(FeCrCu)_{79.1}$ (*b*), $Ni_{24.2}Co_{13.7}(FeCrAl)_{62.1}$ (*c*), $Ni_{9.5}Co_{8.2}(FeCrMn)_{82.3}$ (*d*), $Ni_{25.5}Co_{13.4}(FeCrTi)_{61.1}$ (*e*), $Ni_{16.6}Co_{12.2}(FeCrZr)_{71.2}$ (*f*), $Ni_{21}Co_{12}(FeCrV)_{67}$ (*g*) alloy systems.

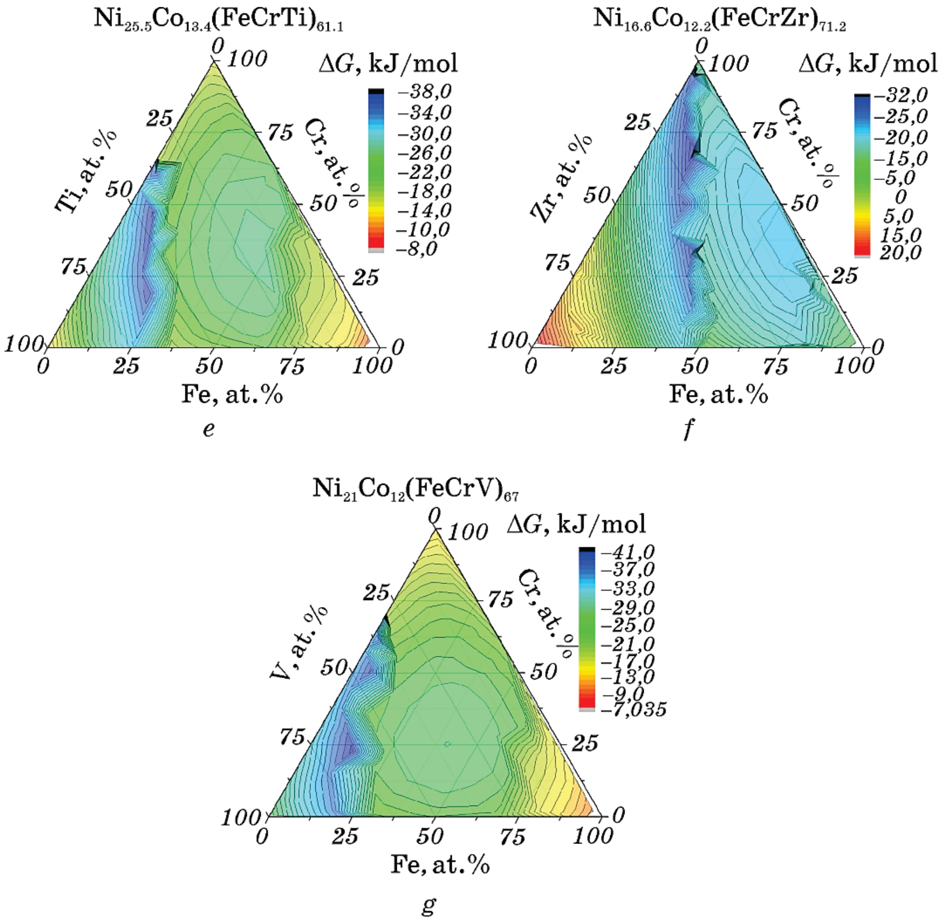

Continuation of Fig. 2.

are formed; when $\Delta G_{intm} << \Delta G_{ssm}$, an intermetallic or intermetallic are formed; when ΔG_{ssm} and ΔG_{intm} have close values, the combination of solid solution and intermetallic compound is formed. To obtain a single-phase homogeneous solid solution, it is advisable to choose compositions with a minimum ΔG_{ss} (Table 3) and the absence of resistant intermetallic.

4. CONCLUSIONS

1. Compositions of alloys based on Ni, Co, Fe, Cr, Cu, Al, Mn, Ti, Zr, V elements with minimal Gibbs free energy are calculated using thermodynamic approach in approximation of regular solid solution model.
2. The solid solution compositions with minimal Gibbs formation ener-

gy considerably differ from equiatomic ones.

3. The compositions of alloys favourable for formation of single phase

TABLE 3. Calculated parameters ΔG, for solid solutions (*ss*) and intermetallic compounds (*int*) with minimal Gibbs formation energy and for residual solid solution (*ss_ss*), (*int_ss*).

No.	Alloys	Solid solutions, Intermetallic	ΔG, kJ/mol	Phase
1	NiCoFeCrCu	*ss*–$Ni_{11}Co_{9.9}Fe_{12.9}Cr_{66.1}Cu_{0.1}$ *ss_ss*–$Ni_{23.9}Co_{24.4}Fe_{23.1}Cu_{28.6}$ *int*–$Ni_{50}Cr_{50}$	−29.145 −10.020 −7.0	*SS* [37]
2	NiCoFeCrAl	*ss*–$Ni_{24.2}Co_{13.7}Fe_{10.9}Cr_{31.3}Al_{19.9}$ *ss_ss*–$Ni_{12.6}Co_{31.2}Fe_{36}Al_{20.2}$ *int*–$Ni_{50}Al_{50}$	−37.0495 −16.544 −22.0	*SS* + *IM* [38]
3	NiCoFeCrMn	*ss*–$Ni_{9.5}Co_{8.2}Fe_{10.2}Cr_{55.1}Mn_{17}$ *ss_ss*–$Ni_{26}Co_{26.7}Fe_{25.6}Mn_{21.7}$ *int*–$Ni_{50}Mn_{50}$	−32.078 −16.827 −8.0	*SS* [27]
4	NiCoFeCrTi	*ss* *int*–$Ni_{50}Ti_{50}$ *int_ss*–CoFeCr	– −35.0 −15.351	*IM* [39]
5	NiCoFeCrZr	*ss* *int*–$Ni_{50}Zr_{50}$ *int_ss*–CoFeCr	– −49.0 −15.351	*SS* + *IM* [40]
6	NiCoFeCrV	*ss*–$Ni_{21}Co_{12}Fe_{9.9}Cr_{17.3}V_{39.8}$ *ss_ss*–$Ni_{19}Co_{28.1}Fe_{30.2}Cr_{22.7}$ *int*–$Ni_{50}V_{50}$	−41.404 −17.929 −18.0	*SS* + *IM* [39]
7	CoFeCrCuMn	*ss*–$Co_{14}Fe_{18.5}Cr_{46.9}Cu_{0.1}Mn_{20.5}$ *ss_ss*–$Co_{24.5}Fe_{21.1}Cu_{34.8}Mn_{19.6}$ *int*–$Co_{50}Mn_{50}$	−29.748 −6.858 −5.0	2*SS* [41]
8	NiFeCrMnTi	*ss*–$Ni_{30.6}Fe_{11}Cr_{15.8}Mn_{13.6}Ti_{29}$ *ss_ss*–$Fe_{37}Cr_{27.9}Mn_{32.1}Ti_{3}$ *int*–$Ni_{50}Ti_{50}$	−38.396 −9.602 −35.0	*SS* + *IM* [27]
9	NiCoFeMnV	*ss*–$Ni_{20.3}Co_{11.5}Fe_{9.5}Mn_{12}V_{46.7}$ *ss_ss*–$Ni_{19.8}Co_{26.3}Fe_{27.9}Mn_{26}$ *int*–$Ni_{50}V_{50}$	−40.521 −17.729 −18.0	*SS* + *IM* [41]
10	NiCoCrMnV	*ss*–$Ni_{22.6}Co_{12.3}Cr_{16}Mn_{10.9}V_{38.2}$ *ss_ss*–$Ni_{17.1}Co_{28.5}Cr_{124.4}Mn_{30}$ *int*–$Ni_{50}V_{50}$	−41.551 −23.1180 −18.0	*SS* + *IM* [41]
11	NiCoFeCrCuTi	*ss*–$Ni_{25.4}Co_{12.8}Fe_{11}Cr_{18}Cu_{0.5}Ti_{32.3}$ *ss_ss*–$Ni_{17.4}Co_{20.8}Fe_{22.7}Cr_{15.2}Cu_{33.9}$ *int*–$Ni_{50}Ti_{50}$	−38.545 −8.647 −35.0	*SS* + *IM* [37]
12	NiCrCuAlMn	*ss*–$Ni_{29.5}Fe_{9.5}Cr_{18}Cu_{0.7}Al_{20.7}Mn_{21.6}$ *ss_ss*–$Fe_{26}Cr_{14.9}Cu_{37.4}Al_{11.4}Mn_{10.3}$ *int*–$Ni_{41.9}Cr_{2.37}Al_{40.6}Mn_{15.2}$	−39.039 −6.472 −22.313	*SS* [42]

Continuation of TABLE 3.

No.	Alloys	Solid solutions, Intermetallic	ΔG, kJ/mol	Phase
13	NiCoFeCrCuAl	*ss*–$Ni_{25}Co_{12}Fe_{11.3}Cr_{30.8}Cu_{0.5}Al_{20.4}$ *ss_ss*–$Ni_{6.8}Co_{22.2}Fe_{23}Cu_{35.7}Al_{12.3}$ *int*–$Ni_{50}Al_{50}$	–37.073 –6.467 –22.0	*SS* [43]
14	NiCoFeCrCuMn	*ss*–$Ni_{6}Co_{5.9}Fe_{16.8}Cr_{47}Cu_{0.1}Mn_{24.2}$ *ss_ss*–$Ni_{22.5}Co_{22.6}Fe_{16.6}Cu_{25.8}Mn_{12.5}$ *int*–$Ni_{50}Mn_{50}$	–31.344 –12.764 –8.0	*SS* [27]
15	NiCoFeCrCuAlV	*ss*–$Ni_{25.9}Co_{17}Fe_{7.3}Cr_{10.3}Cu_{0.3}Al_{15.8}V_{23.4}$ *ss_ss*–$Co_{33.3}Fe_{16.8}Cr_{13.5}Cu_{3}Al_{7.6}V_{25.8}$ *int*–$Ni_{38.1}Al_{35.7}V_{26.2}$	–44.125 –37.805 –25.1427	2*SS* [44]

solid solutions are determined.

4. The character of phase formation in equiatomic alloys is investigated.

ACKNOWLEDGEMENTS

The paper contains some ideas and results acting as a background of the scientific project 'High-strength states as a result of specific interatomic interaction in high-entropy solid solutions with martensitic transformation' (state registration number 0120U000160) within the framework of budget program КПКВК 6541230 'Support for development of priority areas of scientific research' of the N.A.S. of Ukraine for 2020–2021 (agreement No. 1-A as from 16.01.2020).

REFERENCES

1. J.-W. Yeh, S.-K. Chen, S.-J. Lin, J.-Y. Gan, T.-S. Chin, T.-T. Shun, C.-H. Tsau, and S.-Y. Chang, *Adv. Eng. Mater.*, **6**: 299 (2004).
2. J.-W. Yeh, *JOM*, **65**: 1759 (2013).
3. Y. Zhang, T. T. Zuo, Z. Tang, M. C. Gao, K. A. Dahmen, P. K. Liaw, and Z. P. Lu, *Prog. Mater. Sci.*, **61**: 1 (2014).
4. M. H. Tsai and J. W. Yeh, *Mater. Res. Lett.*, **2**: 107 (2014).
5. D. B. Miracle and O. N. Senkov, *Acta Mater.*, **122**: 448 (2017).
6. M. C. Gao, C. Zhang, P. Gao, F. Zhang, L. Z. Ouyang, M. Widom, and J. A. Hawk, *Curr. Opin. Solid State Mater. Sci.*, **21**: 238 (2017).
7. Y. Tan, J. Li, S. Tang, J. Wang, and H. Kou, *J. Alloys Compd.*, **742**: 430 (2018).
8. F. Tian, L. K. Varga, N. Chen, L. Delczeg, and L. Vitos, *Phys. Rev. B*, **87**: 075144 (2013).
9. F. Tian, L. Delczeg, N. Chen, L. K. Varga, J. Shen, and L. Vitos, *Phys. Rev. B*, **88**: 085128 (2013).
10. Prashant Singh, A. V. Smirnov, and D. D. Johnson, *Phys. Rev. B*, **91**, Iss. 22: 224204 (2015).
11. D. Ma, B. Grabowski, F. Körmann, J. Neugebauer, and D. Raabe, *Acta Mater.*,

100: 90 (2015).
12. C. Jiang and B. P. Uberuaga, *Phys. Rev. Lett.*, **116**: 105501 (2016).
13. M. C. Troparevsky, J. R. Morris, P. R. C. Kent, A. R. Lupini, and G. M. Stocks, *Phys. Rev. X*, **5**: 011041 (2015).
14. F. Zhang, C. Zhang, S. L. Chen, J. Zhu, W. S. Cao, and U. R. Kattner, *CALPHAD*, **5**: 1 (2014).
15. C. Zhang, F. Zhang, S. Chen, and W. Cao, *JOM*, **64**: 839 (2012).
16. O. N. Senkov, J. D. Miller, D. B. Miracle, and C. Woodward, *Nature Comm.*, **6** (2015) 6529.
17. U. Mizutani, *Hume–Rothery Rules for Structurally Complex Alloy Phases* (CRC Press: 2010).
18. Y. Zhang, Y. J. Zhou, J. P. Lin, G. L. Chen, and P. K. Liaw, *Adv. Eng. Mater.*, **10**: 534 (2008).
19. Y. Zhang, Z. P. Lu, S. G. Ma, P. K. Liaw, Z. Tang, Y. Q. Cheng, and M. C. Gao, *MRS Commun.*, **4**: 57 (2014).
20. S. Guo, C. Ng, J. Lu, and C. T. Liu, *J. Appl. Phys.*, **109**: 103505 (2011).
21. S. Fang, X. Xiao, L. Xia, W. Li, and Y. Dong, *J. Non-Cryst. Solids*, **321**: 120 (2003).
22. Y. F. Ye, Q. Wang, J. Lu, C. T. Liu, and Y. Yang, *Scr. Mater.*, 104: 53 (2015).
23. A. F. Andreoli, J. Orava , P. K. Liaw , H. Weber , M. F. De Oliveira , K. Nielsch, and I. Kaban, *Materialia*, **5**: 100222 (2019).
24. A. Takeuchi and A. Inoue, *Mater. Sci. Eng. A*, **304–306**: 446 (2001).
25. F. R. Boer, R. Boom, W. Mattens, A. R. Miedema, and A. K. Niessen, *Cohesion in Metals: Transition Metal Alloys* (Amsterdam, North-Holland: 1988).
26. A. B. Melnick and V. K. Soolshenko, *J. Alloy. Compd.*, **694**: 223 (2017).
27. B. Cantor, I. Chang, P. Knight, and A. Vincent, *Mater. Sci. Eng. A*, **375–377**: 213 (2004).
28. F. He, Z. Wang, Q. Wu, S. Niu, J. Li, J. Wang, and C. T. Liu, *Scr. Mater.*, **131**: 42 (2017).
29. L. Ya. Ropyak, I. P. Shatskyi, and M. V. Makoviichuk, *Metallofiz. Noveishie Tekhnol.*, **39**, No. 4: 517 (2017) (in Ukrainian).
30. A. Takeuchi and A. Inoue, *Mater. Trans.*, **41**: 1372 (2000).
31. A. Takeuchi and A. Inoue, *Mater. Trans.*, **46**: 2817 (2005).
32. A. K. Niessen and A. R. Miedema, *Berichte der Bunsengesellschaft für Physikalische Chemie*, **87**, Iss. 9: 717 (1983).
33. *The Periodic Table of the Elements*, http://www.webelements.com.
34. Y. Zhang, Y. J. Zhou, J. P. Lin, G. L. Chen, and P. K. Liaw, *Adv. Eng. Mater.*, **10**: 534 (2008).
35. X. Yang and Y. Zhang, *Materials Chem. Phys.*, **132**: 233 (2012).
36. A. B. Melnick, V. Ya. Beloshapka, and V. K. Soolshenko, *Nanosistemi, Nanomateriali, Nanotekhnologii*, **17**, No. 3: 557 (2019).
37. X. F. Wang, Y. Zhang, Y. Qiao, and G. L. Chen, *Intermetallics*, **15**: 357 (2007).
38. Y.-F. Kao, T.-J. Chen, S.-K. Chen, and J.-W. Yeh, *J. Alloys Compd.*, **488**: 57 (2009).
39. M.-H. Tsai, J.-H. Li, A.-C. Fan, and P.-H. Tsai, *Scr. Mater.*, **127**: 6 (2017).
40. C. Li, J. C. Li, M. Zhao, and Q. Jiang, *J. Alloys Compd.*, **475**: 752 (2009).
41. F. Otto, Y. Yang, H. Bei, and E.P. George, *Acta Mater.*, **61**: 2628 (2013).

42. H.-Y. Chen, C.-W. Tsai, C.-C. Tung, J.-W. Yeh, T.-T. Shun, C.-C. Yang, and S.-K. Chen, *Ann. Chim. Sci. Matér.*, **31**: 685 (2006).
43. C.-C. Tung, J.-W. Yeh, T.-t. Shun, S.-K. Chen, Y.-S. Huang, and H.-C. Chen, *Mater. Lett.*, **61**, Iss. 1: 1 (2007).
44. B. S. Li, Y. P. Wang, M. X. Ren, C. Yang, and H. Z. Fu, *Mater. Sci. Eng. A*, **498**: 482 (2008).